

## Article

# Post-Fault Energy Usage Optimization for Multilevel Inverter with Integrated Battery

Rok Friš \* , Jure Domajnko , Nataša Prosen  and Mitja Truntič 

Faculty of Electrical Engineering and Computer Science, University of Maribor, Koroška Cesta 46, 2000 Maribor, Slovenia; jure.domajnko2@um.si (J.D.); natasa.prosen@um.si (N.P.); mitja.truntic@um.si (M.T.)

\* Correspondence: rok.fris@um.si; Tel.: +386-2-220-7313

**Abstract:** This paper presents a novel sorting algorithm for modular multilevel inverters (MMCs) with integrated batteries, designed to ensure the uninterrupted operation of electric vehicles (EVs) under post-fault conditions. The proposed system structure consists of an MMC with four full-bridge modules per phase, where one module acts as a spinning reserve during normal operation. The algorithm addresses a single switch fault per phase by operating the faulted module in half-bridge mode, ensuring all batteries remain operational and maintaining full power output and battery capacity without any noticeable changes for the vehicle operator. Unlike conventional fault-tolerant strategies that often reduce power output or disable affected modules, the proposed algorithm isolates the faulty switch while preserving system output. This approach avoids derating and eliminates the need for immediate maintenance, enabling the EV to continue operating under fault conditions. Simulation and experimental results validate the effectiveness of the algorithm under a single switch fault scenario, demonstrating its ability to maintain autonomy and consistent power delivery. This work demonstrates a fault-tolerant MMC principle, offering a robust and scalable solution for enhancing reliability and user satisfaction in EV power systems.

**Keywords:** modular multilevel converter (MMC); fault tolerance; redundancy; uninterrupted operation; sorting algorithm



Academic Editors: Pascal Venet and Rui Xiong

Received: 20 January 2025

Revised: 9 March 2025

Accepted: 24 March 2025

Published: 26 March 2025

**Citation:** Friš, R.; Domajnko, J.; Prosen, N.; Truntič, M. Post-Fault Energy Usage Optimization for Multilevel Inverter with Integrated Battery. *Batteries* **2025**, *11*, 125. <https://doi.org/10.3390/batteries11040125>

**Copyright:** © 2025 by the authors. Licensee MDPI, Basel, Switzerland. This article is an open access article distributed under the terms and conditions of the Creative Commons Attribution (CC BY) license (<https://creativecommons.org/licenses/by/4.0/>).

## 1. Introduction

Power converters with redundant functions are essential for critical applications where continuous operation is required. The failure of such applications can result in high financial damage or even loss of life. Redundancy mechanisms ensure that the converter is operational despite internal faults. Redundant modes of operation vary according to the requirements of the application. They can provide safe shutdown of the system, operation in degraded mode, or uninterrupted performance in the event of a fault. Such inverter systems can also be used in electric vehicles, enabling the driver to bring the vehicle to a safe stop, continue driving with reduced power, or maintain normal driving conditions in the event of a malfunction.

This work is focused on a modular multilevel power inverter with integrated battery for electric vehicles [1–4]. The key redundant function of this power inverter is to maintain access to the battery in all modules, even if one switching element in the system phase fails. In the event of an inverter fault, the vehicle retains full access to the battery's capacity, allowing it to continue on a specified route to its destination. Additionally, the inverter ensures uninterrupted operation after a fault, enabling the vehicle to operate at full rated power.

The topology of a multilevel inverter has several advantages compared to conventional two-level inverters [5–7]. By distributing the output voltage across multiple modules, components with lower maximum allowable voltage can be used. Such components are cheaper and more reliable at reduced voltage levels. Since the output voltage consists of multiple levels, the harmonic distortion of the output is also lower. Despite the higher number of switching elements, the operational reliability of this system can be higher than that of two-level inverters. The disadvantages of the applied topology in electric vehicles include increased inverter cost compared to classical designs [8] and greater system complexity. When comparing a modular multilevel inverter with integrated battery to a classical battery pack with a battery management system (BMS), the used structure has a significant advantage, as it can always utilize all the energy stored in the battery cells [9–11]. Classical battery packs shut down when the weakest cell reaches the minimum allowable voltage. In such cases, energy may remain in other cells but cannot be used. The multilevel inverter also supports various redundant operating modes. This can be achieved without additional hardware by adapting the software [12,13] or with additional redundant modules [14,15]. The software method uses a modified modulation technique to mitigate fault occurrence in a module. This is typically achieved by disabling the faulted module and continuing operation without it. However, this method always results in degraded inverter performance due to missing output levels. Alternatively, including redundant modules in the topology can improve fault tolerance. A redundant module can partially or fully replace the faulted one, allowing the inverter to maintain operation. The main disadvantage of additional hardware is the increased cost and volume of the inverter. By integrating the battery into the modules, similar redundancy methods can be achieved. The additional module includes a battery, which is actively used during operation and increases the inverter's autonomy. This minimizes the drawbacks of using a redundant module without a battery. However, the authors of the existing work are primarily focused on the software-based exclusion of a faulted module from the system [16–18], a method that may not be ideal for electric vehicle applications.

The chosen inverter topology consists of full-bridge modules with integrated battery cells [19]. Four modules will be used in each phase of the system, one of which will be redundant. The system will externally operate with a seven-level output, utilizing three active modules. The redundant module will actively participate in the inverter's operation, supplying energy from its battery in the same manner as the other modules. It is crucial to maintain the same battery cell voltage in all modules to ensure the symmetrical operation of the inverter and uniform battery discharge. This balance is achieved through a sorting algorithm, which dynamically assigns each module a role in generating the combined output [20–22]. Modules performing different roles consume different amounts of energy for output generation, enabling the sorting algorithm to balance the discharging batteries with different capacities. The role of the redundant module does not contribute energy to the system's output. Therefore, like other roles, it alternates between the modules within a specified time interval.

In the event of a fault in one of the switching elements within a module, the system must respond appropriately without causing output disturbances that could affect the safe operation of the electric vehicle [23]. This will be achieved by immediately disconnecting the faulted module, diagnosing the fault, and reintegrating the faulted module with partial functionality. If an open-circuit (OC) or short-circuit (SC) fault occurs within the switching element of the full-bridge circuit, a current path between the battery and the output will always remain available. Such a module can operate as a half-bridge, generating either a positive or a negative output voltage. This ensures uninterrupted access to the battery cell, preserving the autonomy of the electric vehicle. However, a faulted module operating in

half-bridge mode can only deliver half of the maximum energy from the battery compared to a fully operational module. To address this issue, an enhanced sorting algorithm will be used to ensure uniform discharge of all battery cells in the modules, including the faulted one.

With the presented approach of using modules in a modular multilevel inverter, redundant operation can be ensured in the event of a fault in a single switching element within a phase of the system. This approach maintains access to all battery cells in the system and ensures the functionally safe operation of the system. Implementing such a strategy in electric vehicles would ensure that, in the event of a fault, the vehicle's autonomy and power remain unchanged.

This paper is organized as follows. In Section 2, following the introduction, the topology description of the used multilevel inverter with an integrated battery is provided. In Section 3, the commonly used sorting algorithm and the improved version are presented. The algorithm operation is described in detail and key improvements are shown. The theoretical derivation of the proposed algorithm is presented in Section 4, demonstrating its feasibility. In the following Section 5, a simulation model of the system was developed and tested using the proposed algorithm. A comparison of results between the basic sorting algorithm and the improved version is provided. Section 6 describes the construction of a modular multilevel inverter with an integrated battery. The simulation results were validated through experimental testing. A discussion of the theoretical, simulation, and experimental results is presented in Section 7. Finally, Section 8 concludes the paper by summarizing the key contributions and outcomes.

## 2. Topology

In the scope of this work, a four-module multilevel inverter topology was selected. In Figure 1, a basic schematic for one output phase is shown. Each module consists of a full-bridge circuit and an integrated battery. The system consists of three standard modules and one redundant module, which functions as a spinning reserve. All modules are identical and operate equally under normal operation. The redundant module H-bridge is not required under normal operation, but its battery contributes to the total battery capacity of the system. In the example presented, a 1/3 battery capacity increase is gained compared to a three-module system without redundancy.

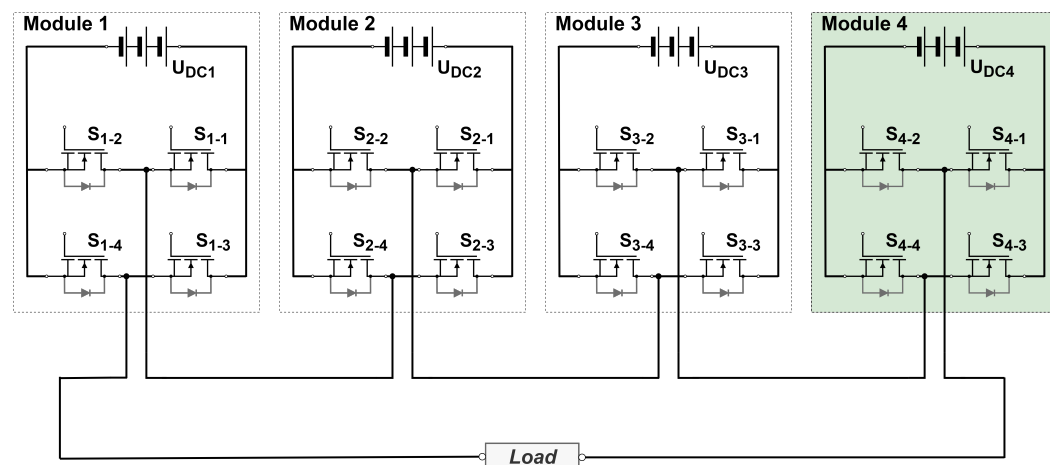


**Figure 1.** Schematic of modular multilevel inverter with integrated battery and a redundant module.

A critical requirement for a stable system operation is maintaining similar battery voltage levels across all modules. Under this conditions, the system will operate in a symmetrical mode. If one module is not able to follow the average module voltage, it will

compromise the system's stability, resulting in asymmetrical operation. This will affect the output waveform and cause deformities in the sine wave. To mitigate this issue, a well-known sorting algorithm is employed to balance the battery voltages across all modules in the system.

The implemented strategy enables redundant operation by simply replacing the faulted module with a redundant one. This method will not affect the operation of the inverter, but disconnecting the faulted module will cause its battery capacity to be lost. To avoid this drawback, a new redundant operation is proposed. Instead of disconnecting the faulted module, it can continue operating as a half-bridge, functioning during either the positive or the negative half-cycle of the waveform. This solution is feasible in cases where a SC or OC fault occurs in one of the switches within the full-bridge. A current path to access the battery can always be found in half-bridge operation regardless of fault location.

### 3. Algorithm

To achieve redundant operation with the topology presented, a suitable algorithm must be used. The sorting algorithm's main function is module voltage balancing in multilevel systems. Redundancy can be added with additional modules, which are used as spinning reserves to maintain similar voltage levels across all modules in the system.

#### 3.1. Module Roles

The sorting algorithm operates in periodic cycles. During each cycle, the battery voltage of each module is measured, and specific module roles are assigned. Each module with an assigned role contributes a different part to the output voltage level of the system. The energy consumption of each module role is different, thus enabling module battery balancing during operation. A visual representation of role assignment and its duration within the system output is shown in Figure 2. The positive half-wave is shown as an ideal filtered voltage form, while the negative half-wave represents the theoretical state. Role operation times are indicated within the system output waveform. Because the redundant module is present in the system, a role 0 is introduced during normal operation. The module assigned to role 0 does not contribute to the system output.

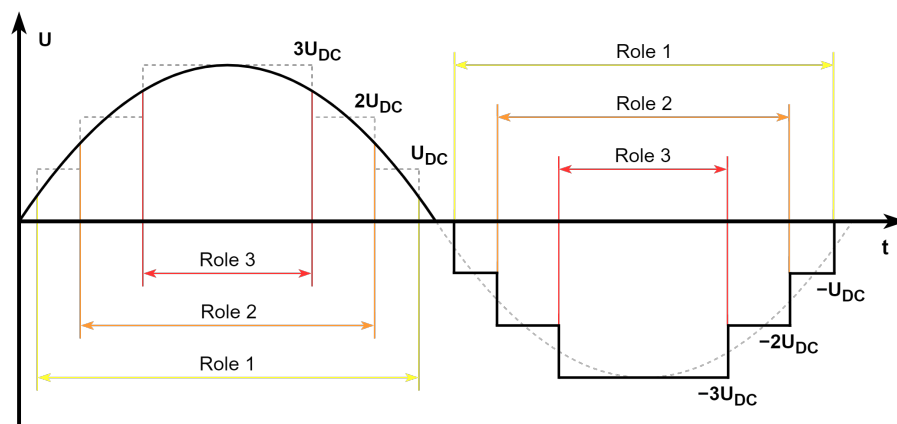


**Figure 2.** Role operation in output voltage.

In each cycle of the sorting algorithm, module roles are assigned according to module battery voltage level. The module with the highest battery voltage is assigned role 1, which consumes the most energy, while the module with the lowest battery voltage will be assigned to role 0 and will not use any energy during this cycle. This allows the algorithm to evenly balance battery usage across modules, even if their capacities are different. The energy consumption by each module operating with a dedicated role is

theoretically calculated by analyzing the sine wave contributions of each module to the overall system output. The output voltage can be treated as a value proportional to the current, thus allowing energy comparison. Figure 3 shows the visual representation of energy consumption for modules operating in different roles, demonstrating the balancing effect achieved through this method. In Figure 3a, the module's energy consumption for role 1 is presented. In Figure 3b, the module's energy for role 2 consists of two sine waves. Finally, in Figure 3c, the energy consumption of the module operating in role 3 is shown.

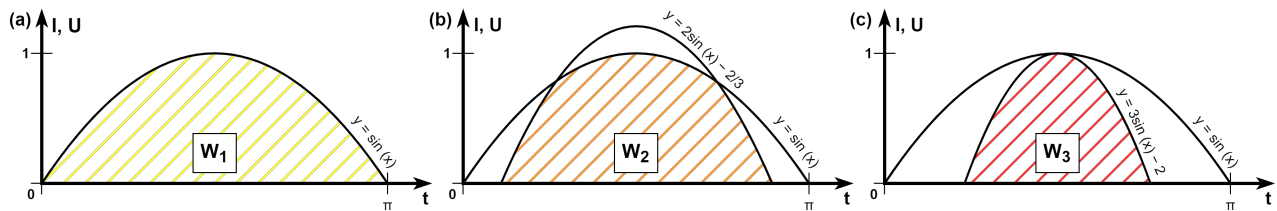


**Figure 3.** Energy consumption for modules operating in different roles: (a) Operating role 1, (b) Operating role 2, (c) Operating role 3.

### 3.2. Improved Sorting Algorithm

The basic sorting algorithm can be improved by including a half-bridge operation mode. This is activated when a single switch fault occurs within a module. Depending on the fault type and position, the improved sorting algorithm allows the faulted module to continue operating as a half-bridge. This method ensures continuous access to the module's battery so the system battery capacity will remain unchanged after the fault. For successful operation with a faulted module, another fully functional module must compensate by covering the missing half-period of the faulted module. Together, both function as one fully functional module and are assigned the same role by the improved sorting algorithm. A comparison between flowcharts of basic and improved sorting algorithm operation is shown in Figure 4. Two additional steps were added to the improved sorting algorithm. The first step determines the fault type and position, including the detection of an OC or SC switch fault and the location of the faulted switching element within the bridge. With this data, the algorithm can decide which half-wave of the faulted module is still capable of generation. The second step determines the module that will compensate the missing half-wave signal, based on the module's battery voltage levels. Finally, role positions need to be adjusted, and role 0 must be excluded from selection.

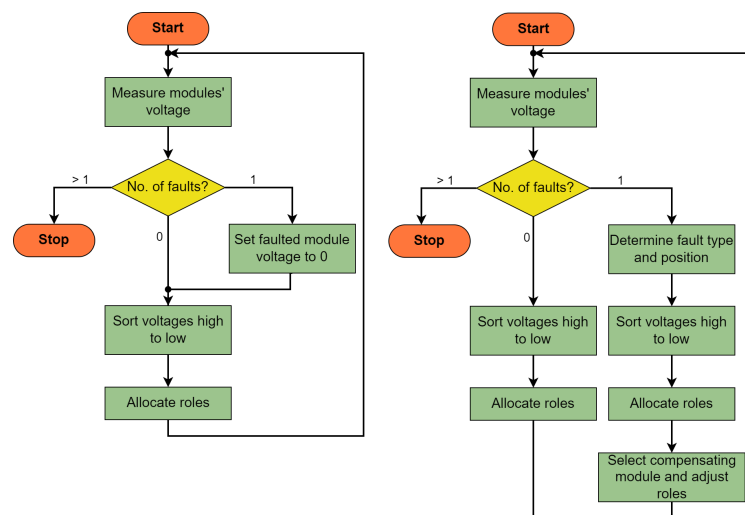


**Figure 4.** Simplified flowchart of basic and improved sorting algorithm.

## 4. Theoretical Derivation

To theoretically verify the proposed improved sorting algorithm, mathematical derivation was used. By calculating the theoretical energy consumption associated with each module role, an energy consumption ratio over a given operational period was determined. This can be used to assess whether or not the module voltage balancing is sufficient for long-term operation.

### 4.1. Energy Ratios

To accurately calculate the energy used by the modules operating in each role, Equations (1)–(3) were used.  $P$  stands for power, or output voltage amplitude, and can vary from 0 to 100%. The sine wave shapes were obtained through modulation scaling to achieve a true sine wave on the system output. Operational role 1 uses the fundamental sine wave,  $\sin(x)$ . Its switching period is active from 0 to  $1/3$  of the system's output voltage for the rising wave. On the timeline, this corresponds from 0 to  $\arcsin(1/3)$ . For the remaining part of the wave, the module with this operating role provides battery voltage at its output without switching. Operation role 2 consists of two sine waves. One is fundamental  $\sin(x)$ , which is used in the non-switching part of the operation. The wave used for switching is scaled accordingly to produce a pure sine wave at the system output. For a three-module system, the wave is scaled to  $2\sin(x) - 2/3$ . Operational role 2 becomes active at  $1/3$  of the system's output voltage, and its switching period lasts until  $2/3$  of the rising wave. On the timeline, these limits correspond to  $\arcsin(1/3)$  and  $\arcsin(2/3)$ , respectively. Operation role 3 operates only in switching mode. The wave is scaled accordingly to ensure a smooth system output, with a reference value following  $3\sin(x) - 2$ . This mode is active from  $2/3$  of the system's output voltage up to 1 for the rising wave, corresponding to  $\arcsin(2/3)$  and  $\pi/2$  on the timeline. The calculations were performed over a half-period of a theoretical sine wave, with  $P$  set to 100%. The areas under the sine wave were calculated, representing the energy consumed by each module. Values  $W_1$ ,  $W_2$ , and  $W_3$  were normalized to present the results in Table 1 as percentages. In half-bridge operation, a module can only contribute energy during either the positive or the negative half-wave, effectively halving the energy output compared to normal operation.

$$W_1 = \int_0^{\pi} P \sin(x) dx = 2 \quad (1)$$

$$W_2 = \int_{\arcsin(\frac{1}{3P})}^{\arcsin(\frac{2}{3P})} \left( 2P \sin(x) - \frac{2}{3} \right) dx + \int_{\arcsin(\frac{2}{3P})}^{\pi - \arcsin(\frac{2}{3P})} P \sin(x) dx + \quad (2)$$

$$+ \int_{\pi - \arcsin(\frac{2}{3P})}^{\pi - \arcsin(\frac{1}{3P})} \left( 2P \sin(x) - \frac{2}{3} \right) dx \approx 1.761$$

$$W_3 = \int_{\arcsin(\frac{2}{3P})}^{\pi - \arcsin(\frac{2}{3P})} (3P \sin(x) - 2) dx \approx 1.108 \quad (3)$$

**Table 1.** Normalized energy consumption of each module role with  $P = 100\%$ .

Module Role	Full-Bridge Operation	Half-Bridge Operation
1	100.0	50.0
2	88.0	44.0
3	55.4	27.7
0	0	0

#### 4.2. Operation Limit

The normalized energy values from Table 1 were used for theoretical validation of the proposed algorithm. The operational limit is determined by the system's ability to consume sufficient energy from a faulted module operating as a half-bridge to keep all the modules battery voltages similar. This condition is expressed in Equation (4). The faulted module assigned to role 1, operating as a half-bridge ( $R1_{HB}$ ), consistently consumes 50% of the energy during each cycle. To compensate for the missing half-wave, a healthy module will be assigned role 1 ( $R1_{HB}$ ) in half-bridge operation. Role 2 ( $R2_{FB}$ ) and role 3 ( $R3_{FB}$ ) are normally assigned to the remaining modules with full-bridge operation. For the improved sorting algorithm to function effectively, the average energy consumption by healthy modules must be less or equal to the energy used by the faulted module. If this condition is met, the faulted module can be assigned different roles to balance the battery voltage.

$$R1_{HB} \geq \frac{R1_{HB} + R2_{FB} + R3_{FB}}{3} \quad (4)$$

By inserting values from Table 1 into Equation (4), the conditions for improved sorting algorithm operation are not met at 100% output voltage amplitude. Reducing the amplitude below 80% ensures the conditions are satisfied. Therefore, a theoretical limit of voltage amplitude exists for successful algorithm operation. This can be found by iterative calculation using Equations (1)–(4), where this limit was determined to be 80.2%. For a visual representation of iterative calculations, Figure 5 is provided. The Y-axis represents the normalized energy used by the left and right parts of Equation (4), while the X-axis shows the increase of  $P$  from 70% to 100%. For successful long-term algorithm operation, the system output must remain below or equal to the crossing point of the two graph lines, as indicated in the figure.

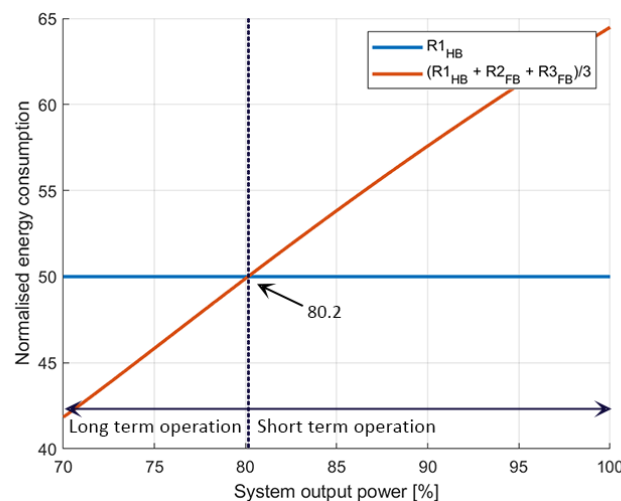


**Figure 5.** Iterative solution for Equation (4).

At this limit, the algorithm will be able to balance the voltage of the faulted module with other modules. The faulted module will be assigned a permanent position with role 1. The maximum power of the system will not be affected, but it will be limited in duration. As long as the battery voltages of the modules remain sufficiently similar, the system can operate above the theoretical limit. However, once the voltage differences exceed acceptable levels, the output power must be reduced to match or fall below the theoretical limit, ensuring stable and balanced operation.

## 5. Simulation Results

The proposed improved sorting algorithm was tested in simulation using Simulink. For this, a theoretical model of a modular multilevel inverter with an integrated battery was built, consisting of four modules where one is redundant. Each module includes a full-bridge with ideal switches, a linear battery, and a PWM controller operating at 20 kHz. The PWM controller is used to control the full-bridge depending on the input information, which is a reference sine wave signal, assigned role from the main unit, and number of active modules in the system. The main unit gathers battery voltage measurements and the fault conditions of modules to execute the sorting algorithm and assigns a role to each. This is executed every period of the reference sine wave. The PWM controller scales the input reference signal according to the number of active modules in the system and offsets the reference signal for a given role to generate a combined system output signal. The main unit chooses between normal or redundant operation depending on the signal from the fault generator unit. This is used to generate a preselected fault type and location at any given time during the simulation. The reference signal of the model is a sine wave at 100 Hz with scaleable amplitude to define the power output. The simulation model is shown in Figure 6. On the left side is the signal part, while on the right is the electrical part. The main unit is connected to all the modules in the system to gather information and control them. The modules operate independently from each other, generating an output determined by the main unit. The electrical part of the simulation model connects all four modules in series to achieve a common multilevel output. For the simulation test, a RL load was used with  $12\ \Omega$  and  $675\ \mu\text{H}$ , and module batteries with 12.6 V. The output voltage amplitude was limited to 80%. A simple linear battery was used in the simulation to achieve a linear discharge curve, following Equation (5). Battery discharge characteristics do not affect algorithm operation.

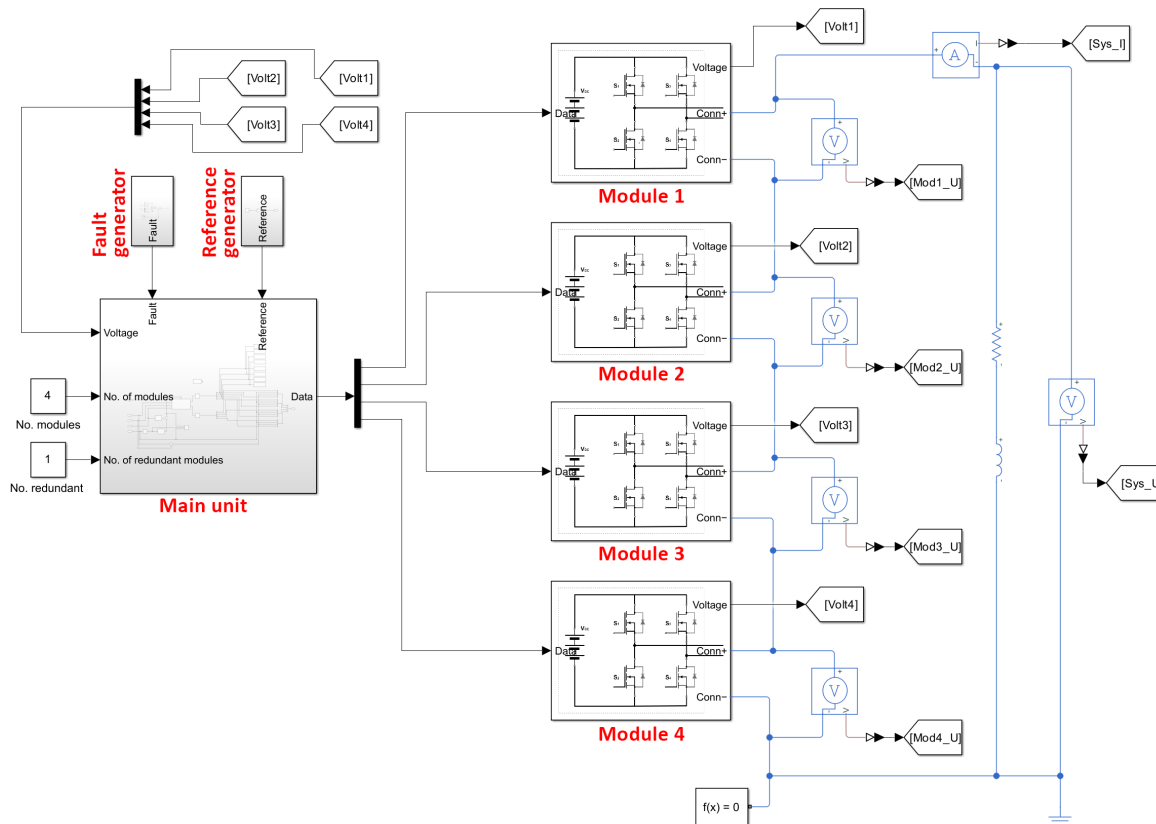


**Figure 6.** Simulation model.

The simulation results of the tested algorithms are presented below. The results are displayed in two formats: first, a detailed view of each module's modulation operating with the assigned role, along with the combined system output; second, an overview of the module battery levels and role assignments during inverter operation.

$$U_{bat} = 12.6 - \frac{1}{25000} \int I(t)dt \quad (5)$$

### 5.1. Basic Sorting Algorithm

To verify the model operation and to compare results, initial tests were conducted using the basic sorting algorithm. In Figure 7, the simulation results of the inverter normal operation are presented over two periods, demonstrating how each module contributes to the overall system output. Figure 7a–d show the voltage output and battery current for each module operating with roles 1, 2, 3, or 0. Role assignment rotates every period to discharge the batteries equally. Because role 0 is present in the system, one module is inactive in each period, contributing no energy to the output. During the first period of the simulation, module 1 was assigned with role 1, module 2 with role 2, module 3 with 3, and module 4 with 0. In the next period, the sorting algorithm measures module battery voltages and changes the assigned roles to balance battery voltages. In the second period of the simulation, module 1 was assigned role 0, module 2 with role 3, module 3 maintained role 3, and module 4 took on role 1. Figure 7e presents the output of the system, which consists of all modules connected in series. The resulting voltage output is 7-level, as three modules are active at any given time, and the remaining one functions as a spinning reserve.

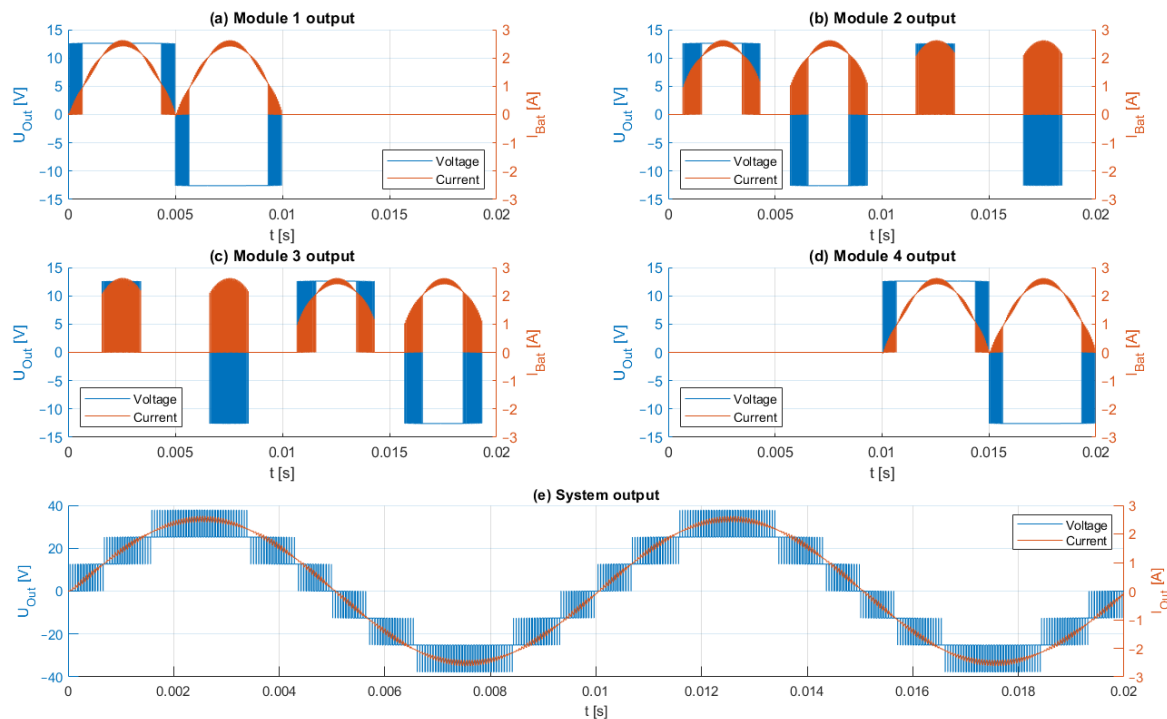


**Figure 7.** Output voltages and currents under normal operation with basic sorting algorithm.

Role assignment of the basic sorting algorithm under normal operation is presented in 20 periods of operation in Figure 8. Since the ideal switches and battery are used, the simulation operation is periodical until one battery reaches its minimum allowable voltage. Figure 8b represents the assigned role to each module, while Figure 8a presents module voltages. Module voltages are oscillating around an average value and are kept close. The sorting algorithm dictates role assignment depending on the module voltage level during

operation. Oscillations occur due to module roles consuming different amounts of energy each period. To compensate for this, the module roles are changed every period. The faster the role switching occurs, the lower the voltage oscillations will be.

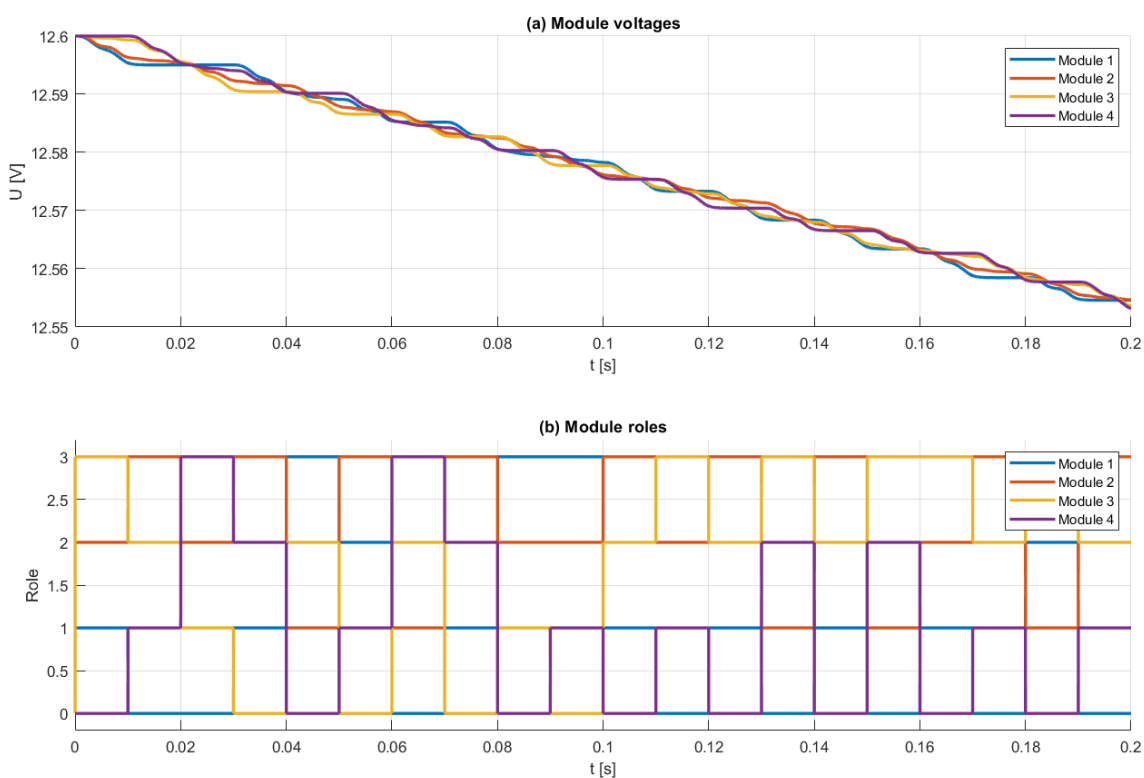


**Figure 8.** Module roles and voltages under normal operation with basic sorting algorithm.

In the event of a fault, the basic sorting algorithm will disable the faulted module by permanently assigning it role 0. In this simulation test, the OC fault was injected into switch  $S_{2-1}$  in module 2 at simulation time 0.06 s. In Figure 9, the module output voltages and battery currents are presented from simulation time 0.06 s to 0.08 s. In Figure 9b, module 2 operation is shown, which is disabled due to the permanent assignment of role 0. The three remaining fully functional modules continue normal operation, assigning roles according to their battery voltages. The system output will remain unchanged in this situation, and inverter operation will not be affected, except for the battery capacity. Since module 2 was permanently disabled due to a fault occurrence, its battery capacity is lost and the system will continue operation at 3/4 of its original battery capacity. Figure 10 provides further insights into module roles and voltages during fault conditions. In Figure 10b, the faulted module 2 was assigned permanent role 0, while the remaining three modules rotated roles to balance their voltages. In Figure 10a, the faulted module 2 voltage stopped decreasing at fault time, and its battery capacity was discarded. The system continues operation with three remaining modules.

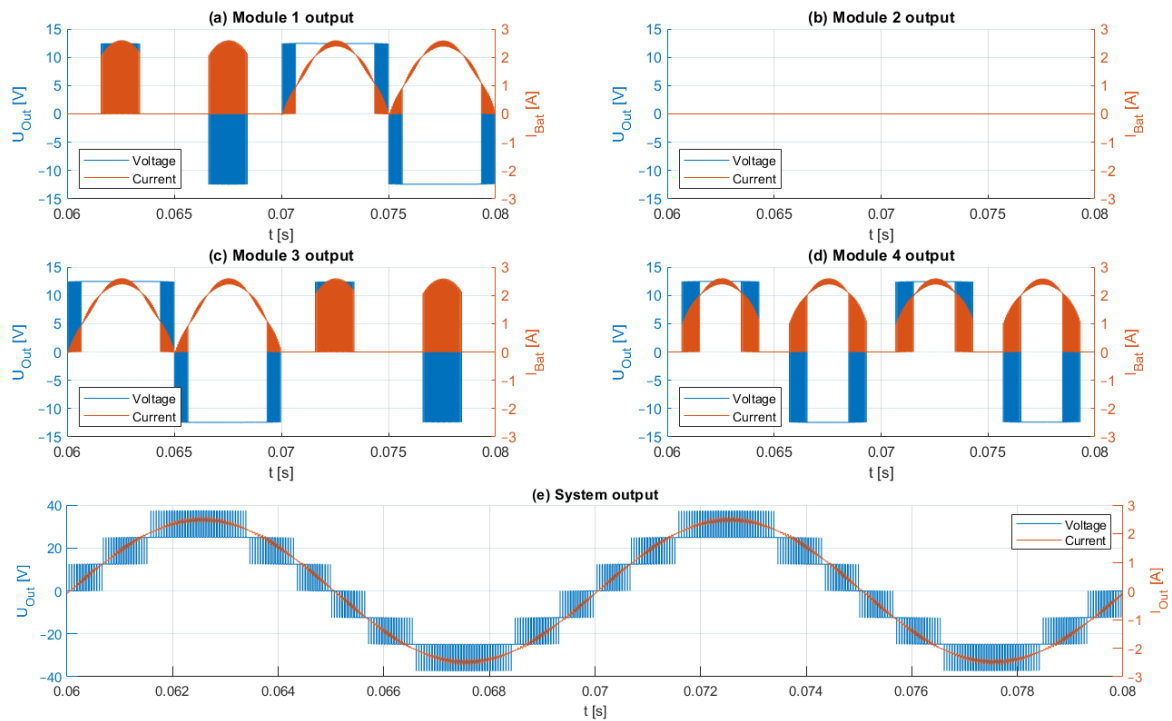


**Figure 9.** Output voltages and currents under fault operation with basic sorting algorithm.

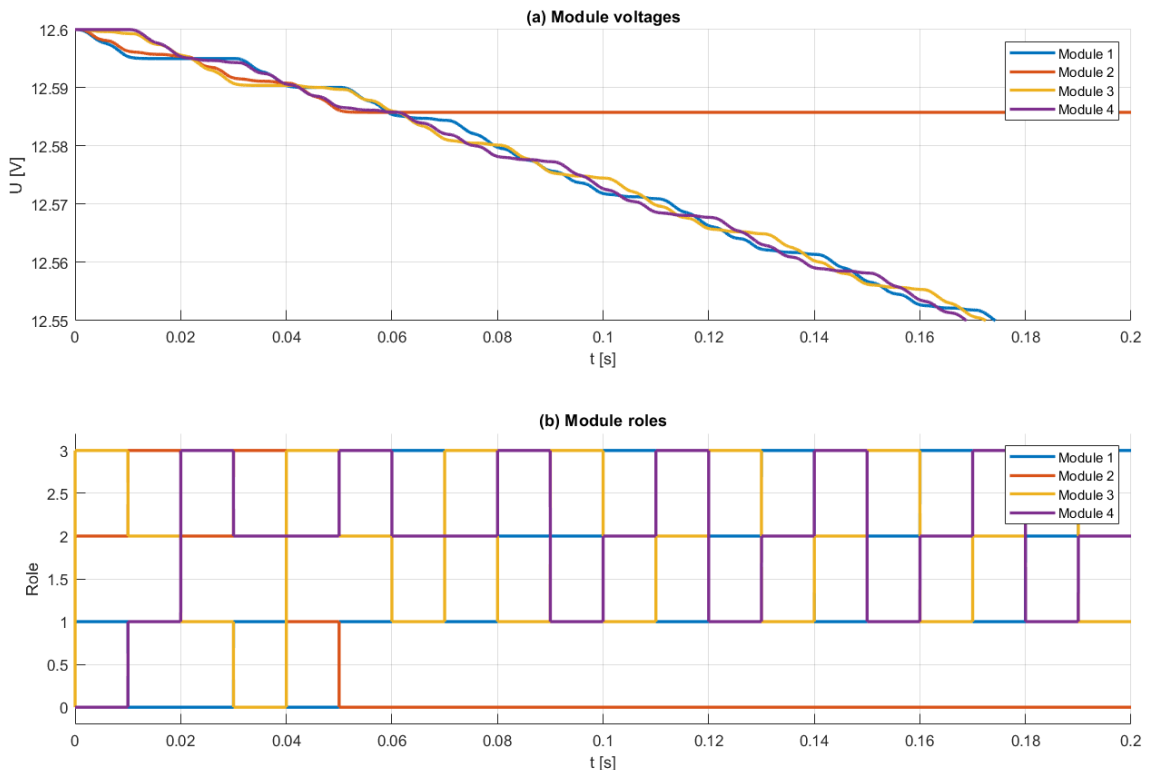


**Figure 10.** Module roles and voltages under fault operation with basic sorting algorithm.

### 5.2. Improved Sorting Algorithm

In the following simulation test, the improved sorting algorithm was used; the other parameters remained unchanged. Under normal operation, the results are identical to the basic sorting algorithm shown in Figures 7 and 8. However, when a fault was introduced,

the improved algorithm allowed module 2 to remain operational by utilizing a half-bridge configuration, unlike the basic algorithm that permanently disabled the module. Keeping access to the faulted module battery results in no change in inverter output voltage under fault operation.

To verify the improved algorithm, an OC fault was injected again into switch  $S_{2-1}$  in module 2 at time 0.06 s. In Figure 11, the output voltages and battery currents of each module are shown from time 0.06 s to 0.08 s. In Figure 11b, the output of module 2 is shown, and half-bridge operation mode is visible, generating only a negative half-wave. To compensate the missing positive half-wave, module 1 was used in the first period, and module 3 fulfilled this role during the second period. The overall system output is identical to the one in Figure 7, confirming that the modified sorting algorithm does not affect the system output.

Additional algorithm operation is shown in Figure 12. In Figure 12b, it reveals that no module is permanently assigned to role 0. Instead, the redundant module compensates for the missing half-wave by adopting the same role as the faulted module during each period. Figure 12a demonstrates that module battery voltages remain closely aligned throughout the operation, confirming the improved algorithm's ability to balance the battery voltages of all modules, including the faulted one. Voltage oscillation patterns change at fault time, but the voltages are kept close and do not drift apart.

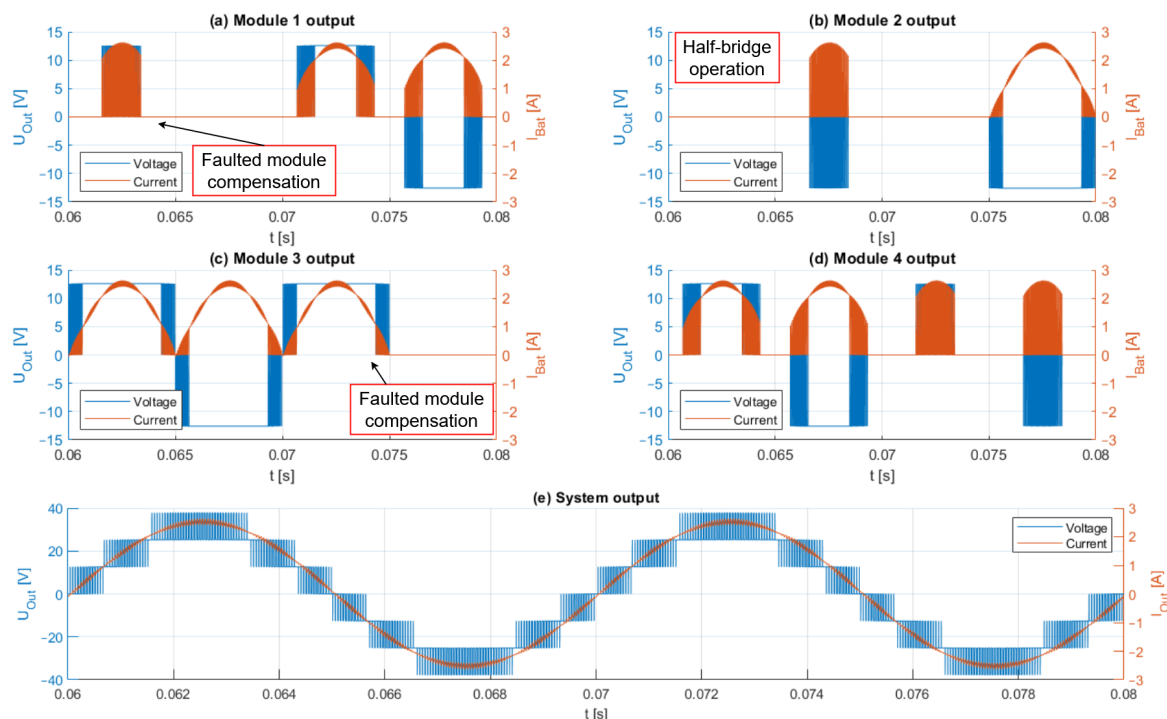


**Figure 11.** Output voltages and currents under fault operation with improved sorting algorithm.

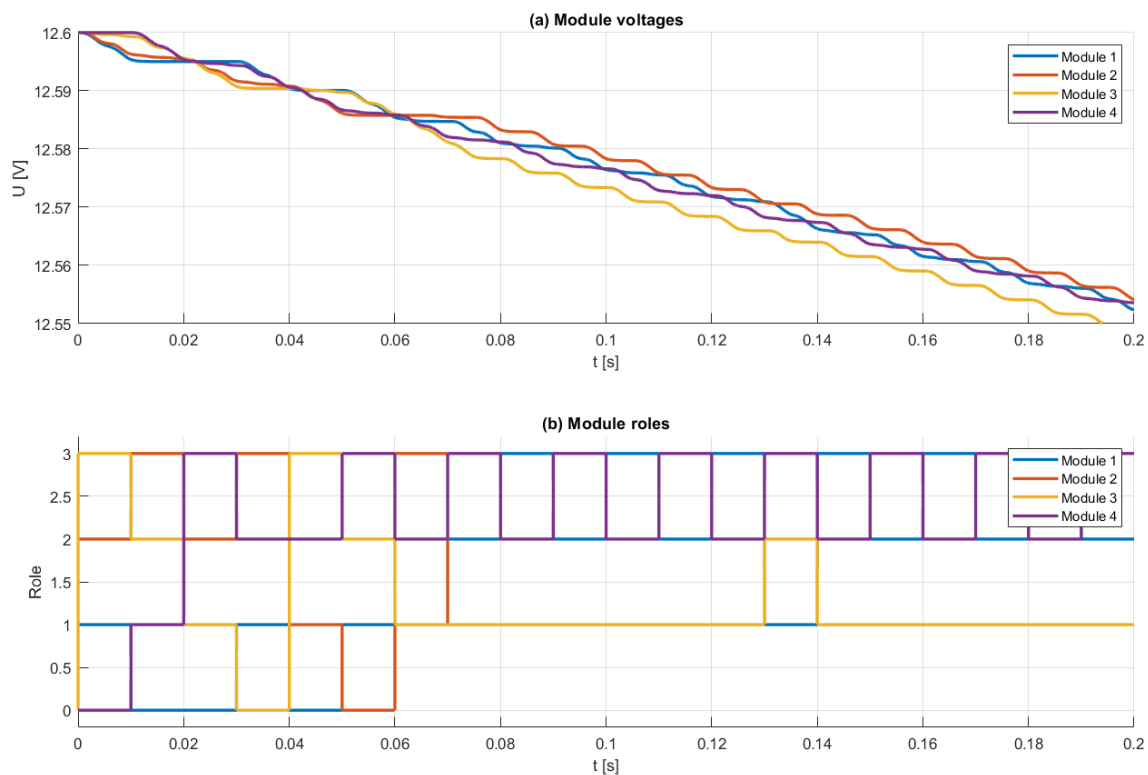


**Figure 12.** Module roles and voltages under fault operation with improved sorting algorithm.

## 6. Experimental Results

An experimental setup was built to further verify the proposed improved sorting algorithm. It was designed for low voltage and low power tests, operating with output currents up to 10 A and a maximum module voltage of 12.6 V. A modular approach was chosen to exchange modules and modify operational parameters easily. The experimental setup is shown in Figure 13, and it consists of six boards, four of which are inverter modules. The backplane is used to create physical power and signal connections for the system. The main unit is the main controller, executing the sorting algorithm. The system communicates primarily via a CAN protocol. For output voltage control, a PWM signal generated by the main unit is used. To synchronize the new role assignment, a dedicated sync signal ensures real-time synchronization. For fast fault communication, four dedicated fault signals minimize the system's reaction time. Voltage and current measurements are performed by each module, and each battery cell is monitored to prevent over-discharging. The measurements are sent to the main unit via CAN, which uses the data to execute the sorting algorithm and assign new roles to each module. When data transmission is complete, the module roles are updated simultaneously with a pulse on the sync signal line. For data logging, a PC running Matlab 2021b was used, and module voltages and dedicated roles were sent to the PC via the UART protocol.

A module contains a full-bridge, three Li-Ion 18650 batteries, a microcontroller, measuring circuits, and safety circuits. Each module operates as an independent unit with operation command signals coming from the system's main controller. All measurement and signal processing is done on board, where only the results are sent to the main controller. The main controller receives operational data from all modules and executes the sorting algorithm at a fixed time period. The results are new role assignments to all modules in the system. Role switching mid operation is performed when all instructions have been sent successfully to the modules, and the reference voltage signal crosses 0 V. This cycle,

presented in Figure 14, repeats every 5 s. The main unit also outputs the reference signal, which is followed by all modules for synchronization and to generate the system output.

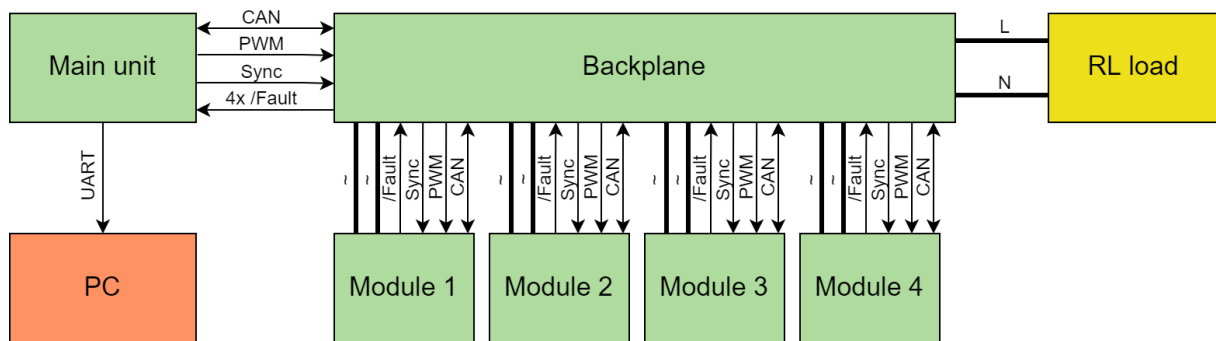


**Figure 13.** Experimental setup diagram.

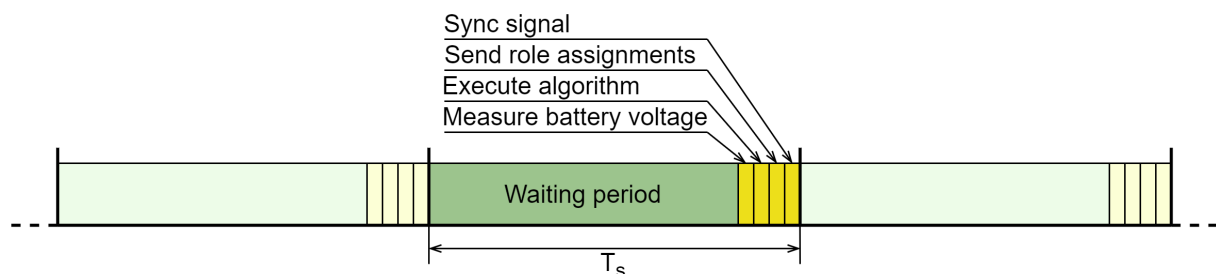


**Figure 14.** Experimental setup operation timeline.

A custom rack was designed to place the modules in the system, as shown in Figure 15, and connect them in series to form a multilevel inverter. The complete system is shown in Figure 16. It contained four modules for single phase operation to perform the test. The system can hold up to 12 modules for 3-phase operation. A RL load was used for the test with  $12\ \Omega$  and  $675\ \mu\text{H}$ , and the output voltage amplitude was limited to 80%, identical to the simulation test.

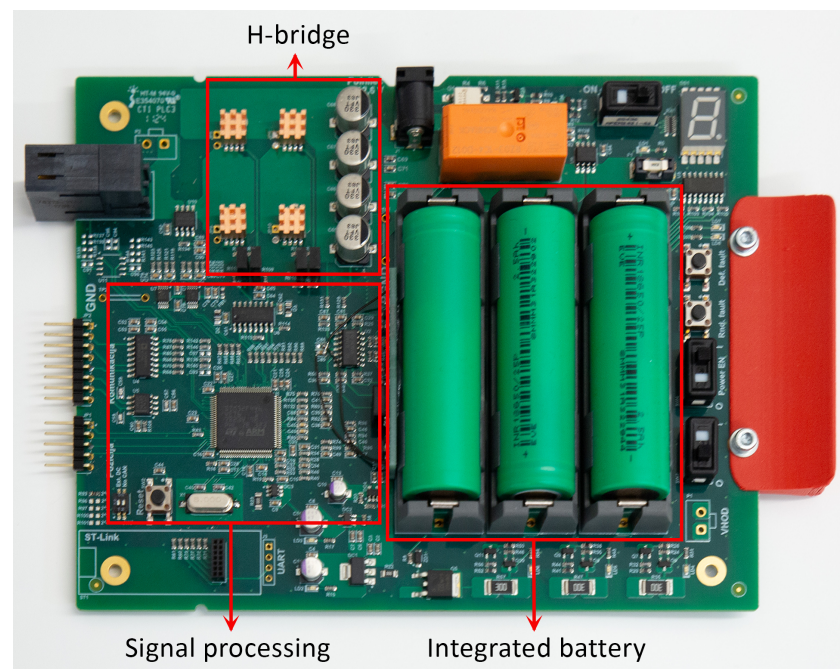


**Figure 15.** H-Bridge module with integrated battery.

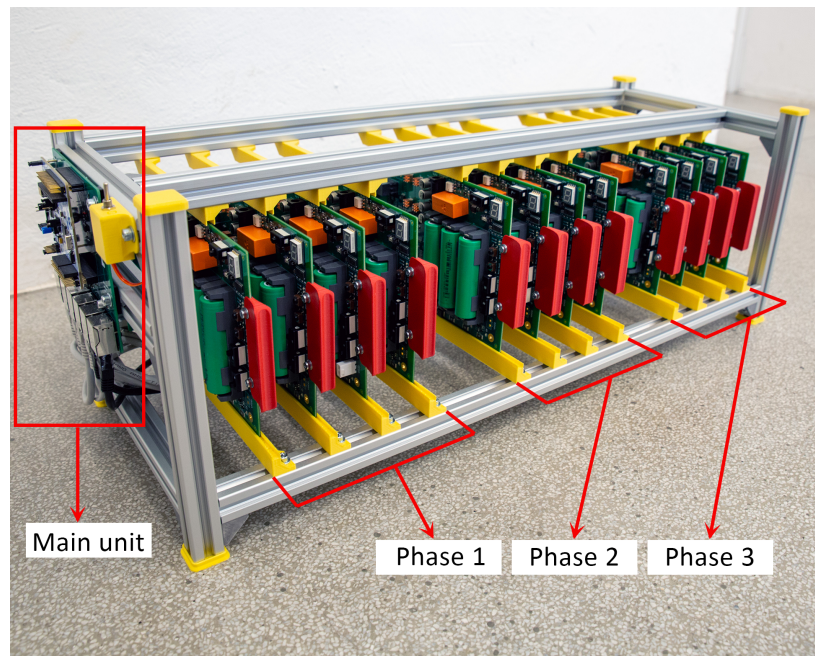


**Figure 16.** Multilevel inverter system with integrated battery.

### 6.1. Basic Sorting Algorithm

The first test was performed using a basic sorting algorithm under normal operation. The test started with full batteries with 4.2 V and lasted until one battery cell in the system reached a minimum voltage level of 3.0 V. In Figure 17, the results are presented in the same format as in the simulation. The first graph shows module voltages, which oscillate around an average value and follow a typical Li-Ion battery discharge curve. The second graph represents module roles. In normal operation, one module acts as a spinning reserve and is assigned role 0. It can be seen that this role is shared among all modules.

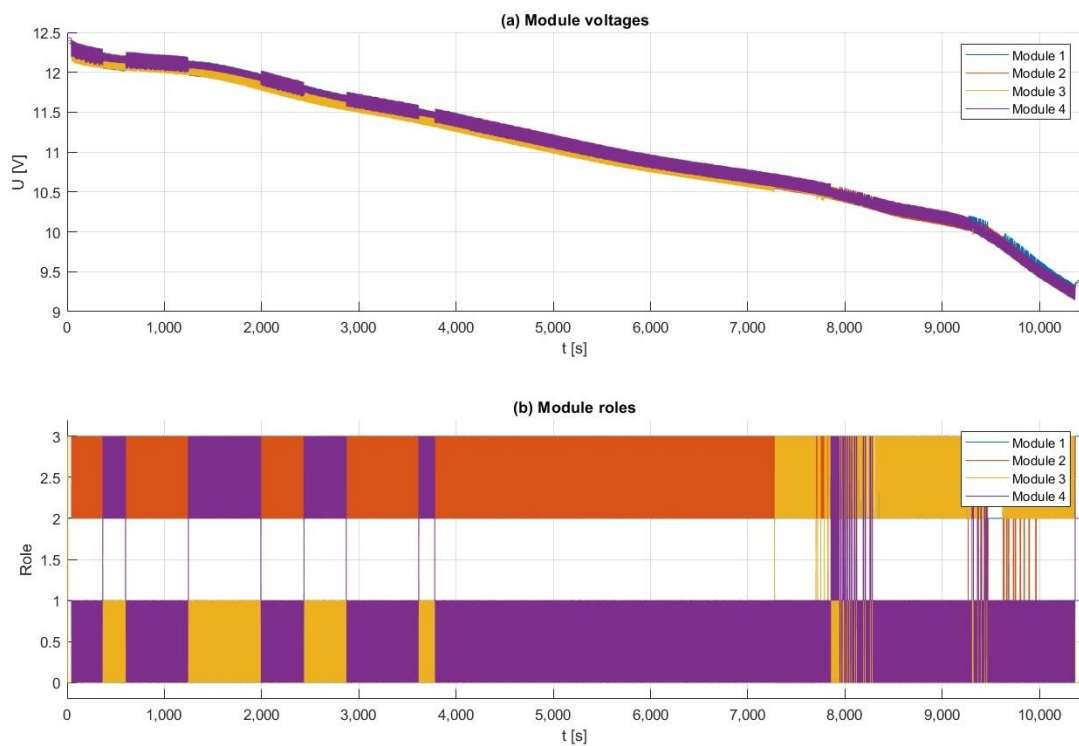


**Figure 17.** Experimental results of module roles and voltages under normal operation using basic sorting algorithm.

## 6.2. Improved Sorting Algorithm

The second test was performed using an improved sorting algorithm under fault operation. Identical to simulation testing, an OC fault was injected into switch  $S_{2-1}$  in module 2 at a test time of approximately 2000 s. In the first graph of Figure 18, the voltage curve remains unchanged after the fault, proving successful battery voltage balancing while using the faulted module. In the second graph, role 0 is no longer used after the fault. The faulted module operates in half-bridge mode and uses another module with the same role to compensate for the missing half-wave in the output voltage.

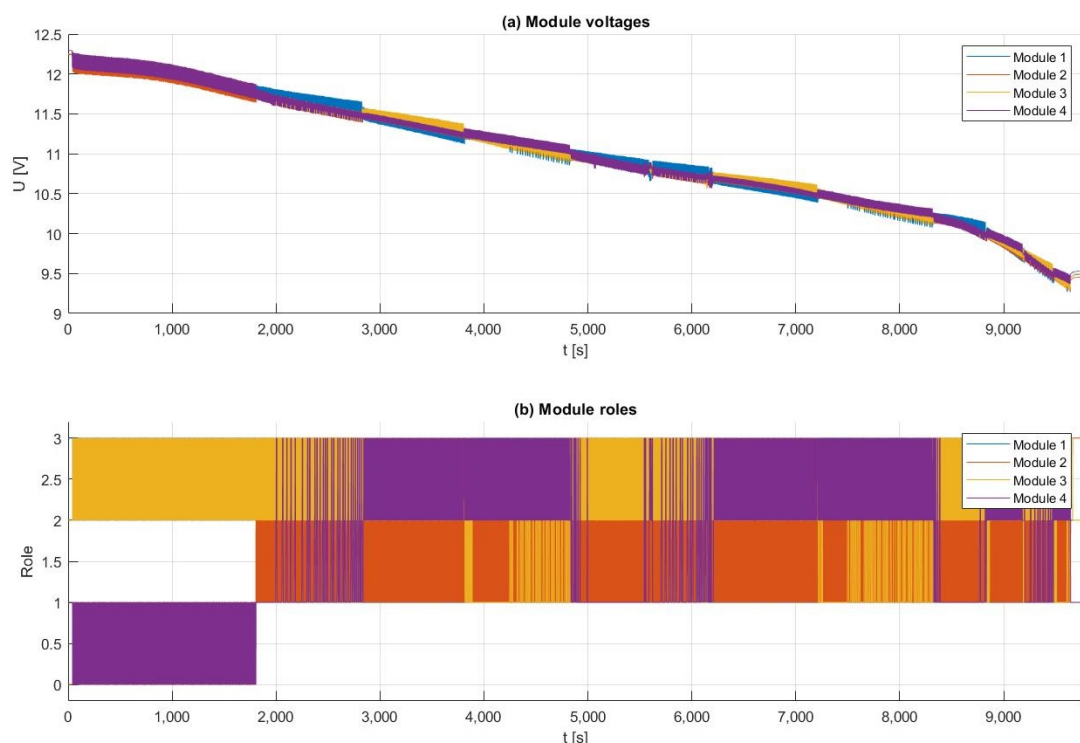


**Figure 18.** Experimental results of module roles and voltages under fault operation using improved sorting algorithm.

## 7. Discussion

In theory, the proposed sorting algorithm was proven successful for use in the redundant functionality of electric vehicles using modular multilevel converters with integrated batteries. However, there is a theoretical operational limit for a constant power output of up to 80.2%, at which the algorithm can operate successfully. For use in electric vehicles, this limit does not pose a significant drawback, since full power is still available for short periods of time. In real-word scenarios, electric vehicles rarely operate at full constant power for long periods of time.

Simulation tests were performed at 80% system power output to show the proposed algorithm operation performance. The first test was performed using the basic sorting algorithm without the fault present, and it is shown in Figures 7 and 8. The goal of this research was to achieve the same inverter performance under fault conditions. In the second test, shown in Figures 8 and 9, the biggest disadvantage of the basic sorting algorithm is shown. If a fault occurs, the faulted module will be discarded from the operation, and its battery capacity will be lost. In this case, the autonomy of the system will be reduced by approximately 1/4 of the original, which the electric vehicle driver will experience as partial range loss. To eliminate this disadvantage, the next test was performed using the proposed improved sorting algorithm with a fault injected into the system during operation.

The results, presented in Figures 11 and 12, show the module voltages being balanced regardless of a fault present in the system. Such system autonomy remains unchanged after a fault occurs, and the electric vehicle driver will notice no difference in vehicle range and short acceleration periods under fault operation.

For final algorithm validation, experimental results were used. In this case, the built modular multilevel inverter system was left operating until one battery cell reached the minimal allowed voltage level. In the first test, the basic sorting algorithm was used, and the results are shown in Figure 17. This test was used as a reference for the second test comparison. The second test was performed using the proposed improved sorting algorithm. The results shown in Figure 18 present the inverter operation under fault conditions. Test time duration remains similar to the first test, which validates the proposed algorithm's successful operation by experimental tests.

The experimental test demonstrated the algorithm's functionality on a low-power, low-voltage system. For realistic application in electric vehicles, the system would need to be scaled up for high-power operation. The functionality of the algorithm is not affected by the voltage or power rating of the system. The experimental test was conducted using a seven-level system with three normal modules and one redundant module. In the example of electric vehicles, a system with more levels could be considered. By increasing the number of output levels and consequently the number of modules, the battery balancing technique becomes easier. An increased number of modules provides more options for the improved sorting algorithm, making the process easier and more accurate. Batteries could be subjected to non-ideal operating conditions, such as cold temperature or aging effects. The algorithm's balancing functionality can balance battery cells with different capacities to some degree, mitigating the negative effects of cell aging and capacity degradation. It can also compensate different battery cell temperatures, and consequently, different available capacities.

In a real-world scenario, an EV operating under fault conditions would not be affected while operating within 80.2% of the system's output power. The vehicle can also operate at full power for a limited duration. This duration is determined by the ratio of the battery capacity to the power the system can provide. The greater the battery capacity relative to output power, the longer the system can operate beyond the 80.2% power limit.

## 8. Conclusions

This paper focuses on developing an improved sorting algorithm applied to modular multilevel inverters with integrated batteries. Targeting electric vehicles as the primary application, the algorithm aims to deliver better redundant functionality in the event of a fault in a single switching element per output phase, by preventing partial range loss. Furthermore, the algorithm is designed to allow full power output for a short duration, ensuring improved reliability and performance under fault conditions.

The proposed improved sorting algorithm demonstrated success in both simulation and experimental systems. Its primary advantage is its superior performance under fault conditions, significantly improving system autonomy compared to a basic sorting algorithm. In the simulation, test duration with and without faults showed no difference in autonomy when using the improved sorting algorithm. However, in experimental tests, a noticeable difference in duration was observed between normal and fault conditions. The test without fault occurrence lasted 10,327 s, while the test under fault conditions lasted 9602 s. The decrease in autonomy is 725 s, which is still significantly lower than when using only the basic sorting algorithm. These results are valid only for the specific battery capacity and power output combination used in the tests. They demonstrate an improvement in operation but indicate the need for further enhancements to the experimental system's

efficiency under fault operation. By implementing the proposed algorithm, a substantial benefit can be gained for electric vehicle performance during fault operations while maintaining unchanged system functionality under regular operation. Furthermore, the implementation of the proposed algorithm requires no hardware modifications to classical multilevel inverters with integrated batteries. The system is scalable to any voltage and power rating and can operate with any number of modules per phase, offering flexibility and applicability in various applications.

Future research could focus on extending the proposed algorithm's operation to a three-phase system. A key challenge in this endeavour would be maintaining balanced phase voltages to ensure symmetrical output while simultaneously balancing the module batteries within each phase under fault conditions. Another aspect of this research could involve increasing the number of modules in single-phase operation and analyzing the impact of these changes on the algorithm's operational limits. The long-term impact on battery health should also be considered. Due to the spinning reserve function, the batteries provide inconsistent energy flow, which might affect their health.

**Author Contributions:** Conceptualization, methodology, investigation, hardware and software design, and writing were performed by R.F.; guidance, supervision, and final review were performed by M.T., J.D. and N.P. All authors have read and agreed to the published version of the manuscript.

**Funding:** This research was funded by the Slovenian Research Agency (Research Core Funding No. P2-0028).

**Data Availability Statement:** All data is available in the article at hand.

**Conflicts of Interest:** The authors declare no conflicts of interest.

## Abbreviations

The following abbreviations are used in this manuscript:

MMC	Modular multilevel converter
EV	Electric vehicle
OC	Open circuit
SC	Short circuit
BMS	Battery management system
PWM	Pulse width modulation
CAN	Controller area network
UART	Universal asynchronous receiver-transmitter

## References

1. Ronanki, D.; Williamson, S.S. Modular Multilevel Converters for Transportation Electrification: Challenges and Opportunities. *IEEE Trans. Transp. Electrif.* **2018**, *4*, 399–407. [[CrossRef](#)]
2. Gan, C.; Sun, Q.; Wu, J.; Kong, W.; Shi, C.; Hu, Y. MMC-Based SRM Drives with Decentralized Battery Energy Storage System for Hybrid Electric Vehicles. *IEEE Trans. Power Electron.* **2019**, *34*, 2608–2621. [[CrossRef](#)]
3. Hariri, R.; Sebaaly, F.; Kanaan, H.Y. A Review on Modular Multilevel Converters in Electric Vehicles. In Proceedings of the IECON 2020—The 46th Annual Conference of the IEEE Industrial Electronics Society, Singapore, 18–21 October 2020. [[CrossRef](#)]
4. Kersten, A. Modular Battery Systems for Electric Vehicles Based on Multilevel Inverter Topologies—Opportunities and Challenges. Ph.D. Thesis, Chalmers University of Technology, Gothenburg, Sweden, 2021.
5. Busquets-Monge, S.; Alepuz, S.; García-Rojas, G.; Bordonau, J. Electric Vehicle Powertrains with Modular Battery Banks Tied to Multilevel NPC Inverters. *Electronics* **2023**, *12*, 266. [[CrossRef](#)]
6. Barros, L.A.M.; Martins, A.P.; Pinto, J.G. A Comprehensive Review on Modular Multilevel Converters, Submodule Topologies, and Modulation Techniques. *Energies* **2022**, *15*, 1078. [[CrossRef](#)]
7. Perez, M.A.; Bernet, S.; Rodriguez, J.; Kouro, S.; Lizana, R. Circuit Topologies, Modeling, Control Schemes, and Applications of Modular Multilevel Converters. *IEEE Trans. Power Electron.* **2015**, *30*, 4–17. [[CrossRef](#)]

8. Roemer, F.; Ahmad, M.; Chang, F.; Lienkamp, M. Optimization of a Cascaded H-Bridge Inverter for Electric Vehicle Applications Including Cost Consideration. *Energies* **2019**, *12*, 4272. [[CrossRef](#)]
9. Xiaofeng, Y.; Zejie, L.; Youyun, W. Modular Multilevel Converter-Based Interphase Distributed Energy Storage System. Patent CN109742780A, 25 January 2019.
10. Slepchenkov, M.; Naderi, R.; Bhakta, M.; Kadri, R.S. Systems, Devices, and Methods for Charging and Discharging Module-Based Cascaded Energy Systems. Patent AU2021256967A9, 13 April 2021.
11. Slepchenkov, M.; Naderi, R. Multi-Phase Module-Based Energy System Frameworks and Methods Related Thereto. Patent US11135923B2, 27 March 2022.
12. Haghnazari, S.; Vahedi, H.; Zolghadri, M.R. Fault tolerant operation strategy design for modular multilevel converters. In Proceedings of the IECON 2016—42nd Annual Conference of the IEEE Industrial Electronics Society, Florence, Italy, 24–27 October 2016; pp. 2172–2176. [[CrossRef](#)]
13. Jiang, Y.; Shu, H.; Liao, M. Fault-Tolerant Control Strategy for Sub-Modules Open-Circuit Fault of Modular Multilevel Converter. *Electronics* **2023**, *12*, 1080. [[CrossRef](#)]
14. Deng, F.; Tian, Y.; Zhu, R.; Chen, Z. Fault-Tolerant Approach for Modular Multilevel Converters Under Submodule Faults. *IEEE Trans. Ind. Electron.* **2016**, *63*, 7253–7263. [[CrossRef](#)]
15. Kim, S.M.; Lee, K.B.; Lee, J.S. Fault-tolerant control scheme for modular multilevel converter based on sorting algorithm without reserved submodules. In Proceedings of the 2018 IEEE Applied Power Electronics Conference and Exposition (APEC), San Antonio, TX, USA, 4–8 March 2018; pp. 223–227. [[CrossRef](#)]
16. Bayati, M.; Tashakor, N.; Farahmandrad, M.; Abkenar, P.P.; Goetz, S. Fault-Tolerant Electric Vehicle Drivetrain with Reconfigurable Battery and Multiphase Machine. In Proceedings of the 2023 IEEE 2nd Industrial Electronics Society Annual On-Line Conference (ONCON), Virtual, 8–10 December 2023; pp. 1–6. [[CrossRef](#)]
17. Sirico, C.; Teodorescu, R.; Séra, D.; Coppola, M.; Guerriero, P.; Iannuzzi, D.; Dannier, A. PV Module-Level CHB Inverter with Integrated Battery Energy Storage System. *Energies* **2019**, *12*, 4601. [[CrossRef](#)]
18. Kucka, J.; Karwatzki, D.; Mertens, A. Optimised operating range of modular multilevel converters for AC/AC conversion with failed modules. In Proceedings of the 2015 17th European Conference on Power Electronics and Applications (EPE'15 ECCE-Europe), Geneva, Switzerland, 8–10 September 2015; pp. 1–10. [[CrossRef](#)]
19. Liang, G.; Farivar, G.G.; Yadav, G.N.B.; Townsend, C.D.; Ceballos, S.; Tafti, H.D.; Pou, J. A Comparison of the Battery Fault Tolerance of Modular Multilevel Converters with Half-Bridge and Full-Bridge Submodules. In Proceedings of the 2021 IEEE Energy Conversion Congress and Exposition (ECCE), Virtual, 10–14 October 2021; pp. 153–159. [[CrossRef](#)]
20. Ma, Y.; Lin, H.; Wang, Z.; Ze, Z. Modified State-of-Charge Balancing Control of Modular Multilevel Converter with Integrated Battery Energy Storage System. *Energies* **2019**, *12*, 96. [[CrossRef](#)]
21. Cai, H.; Hu, G. Distributed Control Scheme for Package-Level State-of-Charge Balancing of Grid-Connected Battery Energy Storage System. *IEEE Trans. Ind. Inform.* **2016**, *12*, 1919–1929. [[CrossRef](#)]
22. Novakovic, B. Modular Multilevel Converters with Module-Level Energy Storage for Medium Voltage Applications. Ph.D. Thesis, The University of Wisconsin, Milwaukee, WI, USA, 2021.
23. Ahmad, A.B.; Ooi, C.A.; Ishak, D. State-of-Charge Balancing Control for Optimal Cell Utilisation of a Grid-Scale Three-Phase Battery Energy Storage System Using Hybrid Modular Multilevel Converter Topology Without Redundant Cells. *IEEE Access* **2021**, *9*, 53920–53935. [[CrossRef](#)]

**Disclaimer/Publisher's Note:** The statements, opinions and data contained in all publications are solely those of the individual author(s) and contributor(s) and not of MDPI and/or the editor(s). MDPI and/or the editor(s) disclaim responsibility for any injury to people or property resulting from any ideas, methods, instructions or products referred to in the content.